publisher
JACS
JOURNAL OF THE AMERICAN CHEMICAL SOCIETY
url
pubs.acs.org/JACS
small
Article

Title
title
A Ferric-Superoxide Intermediate Initiates P450-Catalyzed Cyclic Dipeptide Dimerization

Authors
Hannah E. Gering, Xiaojun Li, Haoyu Tang, Paul D. Swartz, Wei-Chen Chang, and Thomas M. Makris*

references
Cite This: J. Am. Chem. Soc. 2023, 145, 19256−19264
other
Read Online

figure
Image
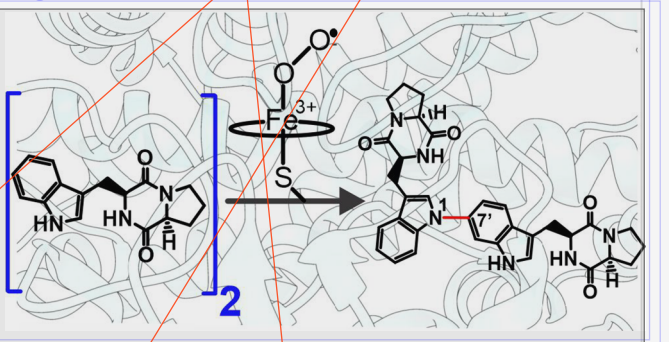

ABSTRACT: The cytochrome P450 (CYP) AspB is involved in the biosynthesis of the diketopiperazine (DKP) aspergilazine A. Tryptophan-linked dimeric DKP alkaloids are a large family of natural products that are found in numerous species and exhibit broad and often potent bioactivity. The proposed mechanisms for C-N bond formation by AspB, and similar C-C bond formations by related CYPs, have invoked the use of a ferryl-intermediate as an oxidant to promote substrate dimerization. Here, the parallel application of steady-state and transient kinetic approaches reveals a very different mechanism that involves a ferric-superoxide species as a primary oxidant to initiate DKP-assembly. Single turnover kinetic isotope effects and a substrate analog suggest the probable nature and site for abstraction. The direct observation of CYP-superoxide reactivity rationalizes the atypical outcome of AspB and reveals a new reaction manifold in heme enzymes.

Headline
INTRODUCTION

Content
The regio- and stereo-selective formation of C-C and C-N bonds represents a fundamental yet synthetically challenging step required for the production of many valuable drugs and agrochemicals. Genome mining efforts have revealed several enzymatic strategies employed by nature to catalyze these reactions for the biosynthesis of important natural products. Arguably, the best characterized class of enzymes known for this type of reactivity are radical S-adenosylmethionine (rSAM) enzymes, which use powerful radical-mediated chemistry to catalyze various types of C-C bond formation and a breadth of other reactions.[1] In addition to rSAMs, the analysis of biosynthetic gene clusters (BGCs) has shown a preponderance of mononuclear heme and nonheme enzymes responsible for catalyzing the oxidative formation of C_{sp2}-C_{sp3}, C_{sp2}-N_{sp2}, and C_{sp3}-N_{sp2} bonds. Inter- and intra-molecular bond formation by cytochrome P450s (CYPs) is prevalent in the biosynthesis of pharmacophores that include phenol cross-link formation during the assembly of glycopeptide antibiotics (GPA) (e.g., teicoplanin and vancomycin)[2−4] and desertorin or orlandin alkaloids,[5] flaviolin dimerization,[6] tryptophan nitration,[7] and amination for indolactam generation,[8] among others. CYPs have also been recently shown to dimerize tryptophan-containing cyclic dipeptides.[9,10]

Tryptophan-linked dimeric 2,5-diketopiperazine (DKP) alkaloids are a large family of natural products that are found in numerous species and exhibit broad and often potent (e.g., antimicrobial and antiparasitic) cytotoxicity.[11,12] One route for dimer biosynthesis consists of a cyclodipeptide synthase enzyme (CDPS) that converts two amino acid charged tRNA molecules to form a cyclic dipeptide.[13,14] CYPs, prevalent in many bacterial CDPS-containing BGCs, have been found to catalyze the downstream dimerization of DKP dipeptides through an oxidative mechanism that has yet to be clarified.[15] One such pathway, shown in Figure 1A, is found in *Streptomyces* sp. NRRL S-1868 and consists of the CDPS AspA that generates cyclo-L-Trp-L-Pro (cWP), also termed brevianamide F. The CYP AspB subsequently forms the N1-C7′-linked dimer termed aspergilazine A (Figure 1A).[16] CYPs that share a very high degree of sequence identity to AspB have been found to catalyze different modes of cWP dimerization, including the C3-C6′ and intramolecular C-N linkage of naseseazine C by NascB.[17] Another recently discovered CYP NzeB was found to have more relaxed regio- and stereo-specificity to form mixtures of both aspergilazine A and naseseazine C.[18,19] The divergent chemoselectivity of CYP dimerases provides an attractive alternative to synthetic routes for late-stage functionalization, particularly for the assembly of asymmetric DKP-dimers.

Despite the prevalence of CYP-catalyzed C-C/C-N bond formation in a number of important natural product biosynthesis pathways, very little is known regarding the enzymatic

headerOrFooter
Received: May 2, 2023
Published: August 23, 2023

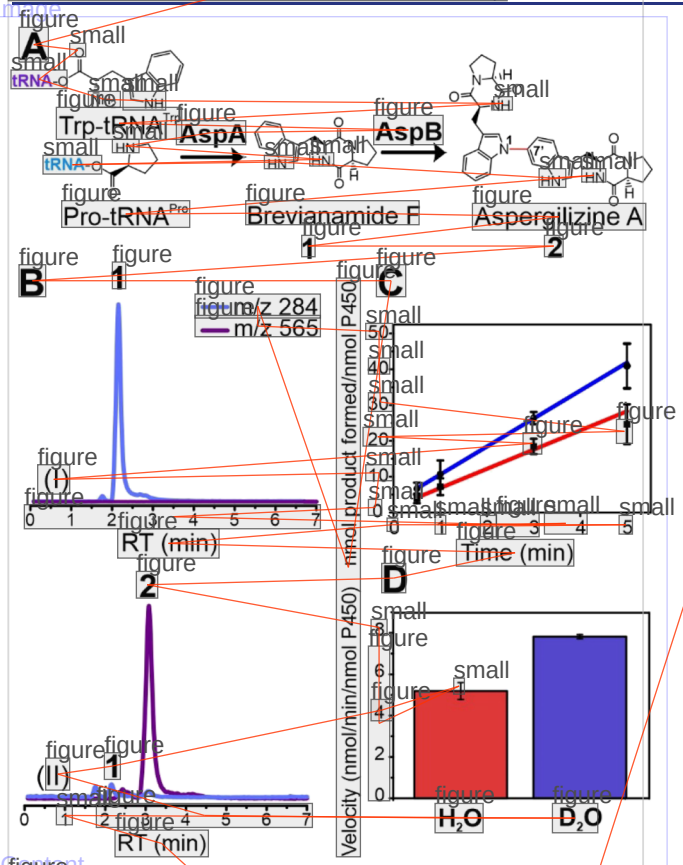

Figure 1. (A) Biosynthetic pathway for aspergilazine A formation by the CDPS AspA and P450 AspB in *Streptomyces* sp. NRRL S-1868. B) $[M + H]^+$ EICs at m/z 284 (light blue) corresponding to the cWP substrate and m/z 565 (purple) corresponding to the dimerized product from prolonged reactions of AspB containing 5 μM AspB, 10 μM sp. FdR, and 25 μM sp. Fd and 200 μM cWP without (I) and with (II) the addition of 1 mM NADPH. (C) Time course of product formation in H_2O (red) and D_2O (blue). (D) Initial velocities of apergilazine A formation by AspB in H_2O (red) and D_2O (blue).

basis for catalyzing a reaction outcome that profoundly differs from the "oxygen addition" (e.g., monooxygenation) reactions that have been the subject of intense scrutiny for many decades. Both radical coupling and cationic pathways have been shown to be energetically plausible, and the most commonly invoked mechanism involves a primary oxidation catalyzed by an iron(IV)-oxo pi cation radical intermediate (compound I, or CYP-I), followed by a secondary oxidation by the resultant Fe^{4+}-OH compound II (CYP-II).[8,20,21] However, direct insight into this process is extremely limited due to the complexity in preparation of the substrates involved (a carrier-protein-linked peptide in the case of GPAs),[3,22] direct access to the fleeting intermediates in the catalytic cycle, or both.

In this study, we use a combination of steady-state and transient kinetics, alternative substrate analogs, and single turnover approaches to evaluate the mechanism for C-N bond formation by the CYP DKP-dimerase AspB. The data provide kinetic and spectroscopic evidence for the unexpected reactivity of an iron-superoxide intermediate for initiating substrate dimerization to form aspergilazine A. We also demonstrate that this reaction trajectory is generalizable to C-C bond formation catalyzed by NzeB. This catalytic strategy rationalizes the circumnavigation of canonical CYP ferryl reactivity to promote selective bond formation that may be extended to the biosynthesis of many other natural products.

RESULTS

Inverse Steady-State Kinetic Solvent Isotope Effect in AspB-Catalyzed Formation of Aspergilazine A. As very little is known about the mechanism for CYP-catalyzed oxidative DKP-dimerization, we sought to explore the basis for C-N bond formation using the DKP dimerase AspB. *In vitro* multiple turnover studies with recombinant AspB and a surrogate redox partner system composed of spinach ferredoxin, ferredoxin reductase (*sp.* Fd/FdR), and NADPH as a source of reducing equivalents resulted in nearly complete consumption of the cWP substrate to form one major product (≥98%) and minor amount of another product with m/z = 565 corresponding to a DKP dimer (Figure 1B). The highly chemoselective profile is in good agreement with prior *in vivo* fermentation experiments by Li et al., which showed that 98% of the substrate was converted to aspergilazine A, while the other ∼2% corresponded to two other DKP dimers with varying linkages.[16] Thus, we assigned the major product peak as aspergilazine A.

The C-N linkage of two molecules of cWP involves a two-electron oxidation of the substrates, and mechanisms that are initiated by indole or DKP N-H abstraction by CYP-I have been advanced.[18,19,23] A structural alignment of AspB with other well-characterized CYP monooxygenases shows a distinct alteration of residues at the I-helix that are known to be critical for O-O heterolysis in O_2-activating CYPs (Figures S1A,B). Notably, AspB lacks the highly conserved acid (Asp or Glu) on the I-helix distal pocket that forms half of the "acid-alcohol pair" that is crucial for mediating proton delivery to the ferric peroxo-anion intermediate (Figure S1C).[24−28] Due to this deviation (a proline is found at the corresponding position in AspB), we performed steady-state kinetic solvent isotope effect (KSIE) experiments to determine if an alternative mode of proton-delivery was operant. A comparison of the rates of product formation by AspB in H_2O and D_2O buffers revealed an *inverse* KSIE of 0.66 ± 0.1 (Figure 1C,D). This phenomenon is highly unusual for a P450 that employs CYP-I as an oxidant, as rate-limiting proton-transfer steps are involved in its generation.[29] Furthermore, increasing the concentration of protons in AspB reactions by lowering the pH resulted in a slower rate of product formation (Figure S2). This is the opposite trend from what was previously observed for the analogous I-helix acid mutant (D251N) in the camphor monooxygenase CYP101.[28] In that case, an increase in the turnover rate and corresponding ∼5-fold increase in the KSIE at lower pH was attributed to an extended proton-delivery chain involved in the generation of CYP-I. In contrast, the availability of protons appears to impede product formation in AspB despite the absence of an I-helix acid.

Inverse KSIEs have been reported for some atypical P450 reactions and used as a rationale to invoke intermediates that precede compound I.[30] These include substrate transformations that are either postulated or demonstrated to be mediated by a ferric-peroxoanion species, such as the 17,20 lyase chemistry catalyzed by CYP17A1 in the conversion of 17-hydroxypregnenolone to dehydroepiandrosterone,[31] and more recently, an epoxide ring-opening cascade of tirandamycin L by mutants of the CYP TamI.[32] However, the nucleophilicity[33] of a ferric peroxoanion complex would make it unlikely to serve as an effective reagent for cWP dimerization.

Transient Kinetic Studies. To gain insight into the potential involvement of an alternative oxidant in AspB, we

https://doi.org/10.1021/jacs.3c04542
J. Am. Chem. Soc. 2023, 145, 19256−19264

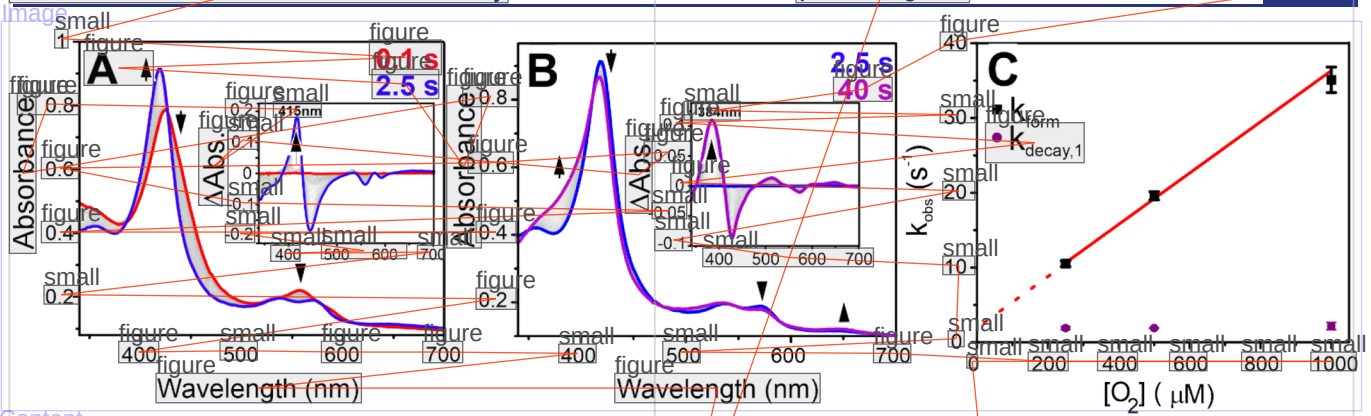

Figure 2. (A) Stopped-flow photodiode array (PDA) spectra depicting the decay of oxy from 0.1 s (maximum oxy formation, red trace) to 2.5 s to the apparent low-spin (LS) complex (blue trace) upon rapid mixing of the enzyme:substrate complex with O_2-saturated buffer at 4 °C. Inset: the difference spectrum with the 0.1 s trace set as the baseline. (B) PDA spectra from the same dataset as A depicting the slow decay of LS at 2.5 s (blue trace) to the high-spin (HS) species at 40 s (purple trace). Inset: the difference spectrum with the 2.5 s trace set as the baseline. (C) Observed rate constants as a function of O_2 concentration for the formation (black squares) and primary decay (purple circles) phases of the oxy complex monitored at 440 nm. The slope of the linear fit of the formation phase of oxy provides the forward rate constant (k_1 = 34.3 ± 2 mM^{-1} s^{-1}) and the *y*-intercept gave the reverse rate constant (k_{-1} = 2.1 ± 0.8 s^{-1}) for O_2 binding. The subsequent decay phase of oxy remained independent of O_2 concentration.

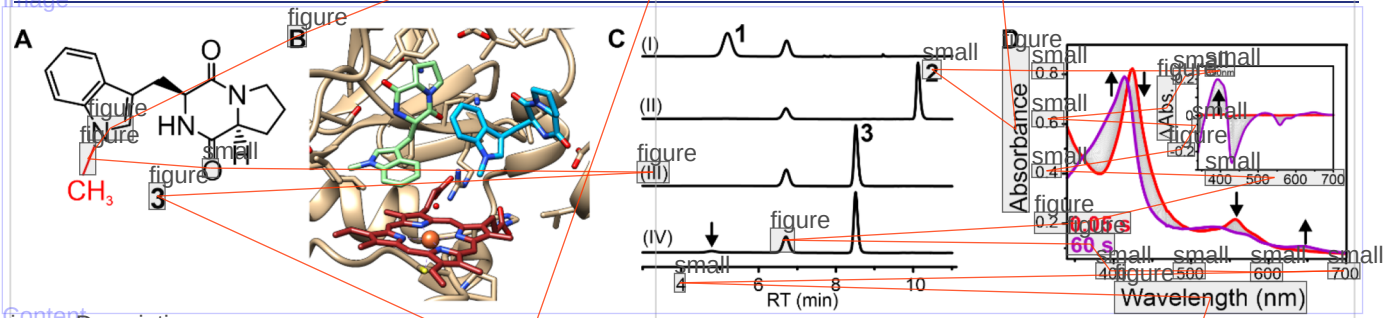

Figure 3. (A) Structure of the *N*1-methyl cWP probe (**3**). (B) Crystal structure of AspB bound to *N*1-methyl cWP. The first and second substrate molecules are shown in blue and light green, respectively. The heme (red) is shown in the low spin state, with a water molecule (red sphere) occupying the 6th coordination site. (C) HPLC traces monitored at 280 nm of (I) 5 μM AspB in the presence of 10 μM sp. FdR and 25 μM sp. Fd reacting with **1** in the absence (I) or presence (II) of 1 mM NADPH over the course of 30 min showing complete conversion of cWP to **2**, and AspB with **3** and sp. Fd/FdR under the same conditions as above in the absence (III) and presence(IV) of NADPH displaying only minor conversion of **3** to a new metabolite, indicated by the arrow. (D) Stopped-flow PDA spectra from 0.05 to 60 s acquired upon rapid mixing of ferrous *N*1-methyl cWP-bound AspB with oxygen-saturated buffer depicting the direct decay of the oxy complex to HS ferric AspB. Inset: the difference spectrum with the 0.05 s trace set as the baseline.

performed stopped-flow absorption experiments at 4 °C where the reduced enzyme-substrate (E-S) complex was rapidly mixed with excess O_2. The resulting ferric-superoxide (or "oxy") complex represents the last semistable intermediate in CYP catalysis and the first branchpoint between productive catalysis and uncoupling. The intermediate can either decay via the release of superoxide via autoxidation, or if a second reducing equivalent is suitably provided, be further activated to form a (hydro)peroxo or CYP-I following the O-O bond cleavage. In the first 100 ms after mixing of the reduced substrate-saturated AspB with excess O_2, the ferrous enzyme rapidly decays to form a new species (Figure S3) with absorption characteristics (Soret λ_{max} ~424 nm and merged Q-bands ~556 nm and a shoulder ~585 nm) (Figure 2A) that are similar to other reported CYP-oxy (Fe^{3+}-O_2^{-}) complexes (Table S1). As a second electron is not provided for catalysis to occur, one would anticipate that autoxidation should result in reformation of the ferric enzyme-substrate bound resting state. Substrate-saturated AspB is composed of a mixture of high- and low-spin (HS and LS) species (~15% HS at 4 °C) (Figure S4). However, the AspB oxy-complex appears to directly decay to a purely LS-form from 0.1 to 2.5 s (Figure 2A) with optical features that closely resemble the substrate-free ferric resting state (Figure S5), before slowly returning to the original mixture of HS and LS species over the following 40 s (Figure 2B, Figure S5). Analysis of the timecourse for cWP-bound oxy-AspB formation and decay at 440 nm required fitting to a three summed exponential (Figure S6). A single rate of formation ~28.1 s^{-1} and two decay phases (2.2 and 0.04 s^{-1}) (Table S2) represent the primary decomposition of the oxy-ferrous species to the initial LS-species and the subsequent slower generation of the enzyme-substrate complex. Evaluation of the kinetics of oxy formation and decay with varying O_2 concentrations show that only the first kinetic phase (oxy-formation) is O_2-dependent as expected, while the latter phases are independent of O_2 concentration (Figure 2C). Further comments on the assignment of each of these phases are provided in the Supporting Information Methods, Figure S7, and Tables S2 and S3.

The direct transition of Fe^{3+}-O_2^{-} to a pure LS species is atypical for substrate-bound CYPs[34−36] and suggests a process that is more complex than autoxidation. Nonetheless, we have previously observed similar behavior in the H_2O_2-dependent CYP OleT.[37] In that case, autoxidation, which ultimately

https://doi.org/10.1021/jacs.3c04542
J. Am. Chem. Soc. 2023, 145, 19256−19264

furnishes H_2O_2, can react with the ferric-heme to initiate catalysis. However, AspB is unable to effectively metabolize cWP using a peroxide-shunt pathway (Figure S8), and the inclusion of catalase did not alter the kinetic behavior for oxy-decomposition, unlike what was found for OleT (Figure S9). Another notable deviation from typical CYP behavior is seen when comparing the decay rates of the oxy-complex for the substrate-bound and free enzyme. In the absence of the substrate, AspB-oxy decays directly back to the ferric resting state (Figure S10). For many CYPs, a bound substrate typically extends the lifetime of the first dioxygen intermediate, occasionally upward of 100-fold,[38] thus allowing second electron transfer event to occur and minimizing the generation of reactive oxygen species. However, there is no significant difference in the decay rate constants for AspB decomposition in the presence or absence of the substrate (2.2 ± 0.3 s^{-1} for substrate-free oxy).

N-Methylated Substrate Derivative Stabilizes the Oxy Complex. We synthesized a substrate derivative where the indole nitrogen was methylated, termed *N*1-methyl cWP (**3**) (Figure 3A), as computational studies by Sherman and colleagues have suggested that DKP-dimerization by AspB may be afforded by primary indole N-H abstraction.[19,23] AspB displayed very similar binding characteristics (K_D and maximal spin-state conversion) with (**3**) (Figure S11). The crystal structure of *N*1-methyl cWP-bound AspB (PDB: 8TWU) was solved to 1.86 Å resolution (Figure S12A, Table S4). As in the crystal structure of AspB bound to cWP (PDB 7S3J), two molecules of (**3**) are found bound in the active site in close vicinity to the heme cofactor (Figure 3B). The first substrate molecule, shown in blue, displays some minor structural differences from that of the native substrate (Figure S12B). This substrate molecule loses some of the concavity seen with the native substrate, and the DKP nitrogen is no longer within hydrogen bonding distance of the heme propionate group as is seen in the crystal structure with (**1**). Nonetheless, the introduced methyl-group is oriented ∼4 Å from the heme-iron in a position that would appear primed for oxidation (e.g., hydroxylation followed by spontaneous demethylation)[8] by an activated oxygen species if it was generated. The second substrate molecule, shown in light green, binds very similarly to what was observed in the crystal structure of the native substrate. HPLC characterization of AspB turnover with (**3**) revealed that the substrate analog was highly inhibitory (Figure 3C) and only produced a very minor amount (∼2%) of a demethylated dimerized product with an m/z = 579 (Figure S13).

As AspB appears unable to effectively metabolize the N-methylated substrate despite a similar binding mode, we compared the spectral and kinetic characteristics for oxy-AspB decay in the presence of **3**. Dramatically different kinetic behavior was observed, as the oxy-complex decayed directly to a mixture of ferric HS/LS states with a composition that was identical to the resting substrate-bound state (Figure 3D) with clearly defined isosbestic points for the transition. While the formation of AspB-oxy was significantly faster in the presence of **3** (238 s^{-1}) with an on rate for O_2 binding ∼3-fold higher than with **1** (Figure S14), the decay kinetics were much slower than cWP and dominated by the amplitude of the slow phase. The rates of both decay phases closely resembled formation of the E-S complex monitored at 390 nm (Figure S15, Table S5), unlike what was observed with **1**. Thus, alteration of the indole moiety of the substrate reverts AspB to the typical autoxidation behavior characteristic of most CYPs.

Provision of a Second electron Is Not Required for Catalysis. Taken together, the unusual behavior for the decay of the AspB-oxy complex in the presence of **1** as well as the inverse KSIE on product formation prompted us to examine the possibility that the generation of CYP-I may not be required for catalysis. The dithionite-reduced E-S complex was exposed to O_2, and samples were then analyzed for product formation. It is unlikely that excess dithionite would be able to effectively reduce the oxy complex, as CYPs prototypically require an allosteric effector role provided by a biological redox partner for efficient second electron transfer.[39,40] Nevertheless, we further excluded this possibility through the removal of excess dithionite by anaerobically desalting the E-S complex following reduction such that only one electron equivalent was provided. Irrespective of this chromatographic step, we observed the efficient formation of a product with identical retention time (Figure 4A), UV-absorption profile and m/z as

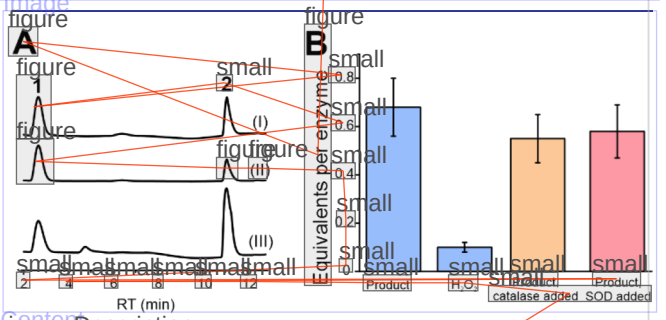

Figure 4. (A) LC-PDA traces monitored at 300 nm of products obtained from reactions of reduced cWP-bound AspB with O_2 (I), reduced cWP-bound and desalted AspB with O_2 (II), and cWP-bound AspB with sp. Fd/FdR and NADPH (III). (B) Quantification of product and H_2O_2 equivalents per enzyme in single electron turnover experiments (blue bars), and quantification of product equivalents per enzyme in the presence of the catalase (orange bar) or SOD (red bar).

2 (Figure S16). The addition of catalase or superoxide dismutase (SOD) did not significantly affect the accumulation of product in single-turnover experiments, ruling out that product was formed via a H_2O_2 shunt pathway or from the reaction of released superoxide to the ferrous enzyme (Figure 4B). Quantitation of the product revealed a highly efficient process, resulting in 0.68 ± 0.12 molar equivalents of **2** per enzyme, while 0.1 ± 0.02 equivalents of H_2O_2 per enzyme was also produced (Figure 4B), accounting for nearly all (∼90%) of the O_2 and redox equivalents provided during the experiment. We were unable to observe any product in single-turnover experiments when **3** was used as the substrate, and H_2O_2 quantitation indicated significantly more H_2O_2 was generated, consistent with the autooxidation behavior shown in stopped-flow experiments (Figure S17).

Evidence for HAT by a CYP Ferric Superoxide. To further probe the nature of the AspB-oxy reaction with the native substrate, we compared the rate of decay of the intermediate under single turnover conditions in stopped-flow experiments in H_2O and D_2O. As both the DKP and indole N-H protons are exchangeable in solvent, we preincubated the E:S complex in deuterated buffer to achieve deuteration at both sites. We observed a normal solvent kinetic isotope effect (k_H/k_D) of 2.6 ± 0.3 (Figure 5A, Table S6), in stark contrast to

https://doi.org/10.1021/jacs.3c04542
J. Am. Chem. Soc. 2023, 145, 19256−19264

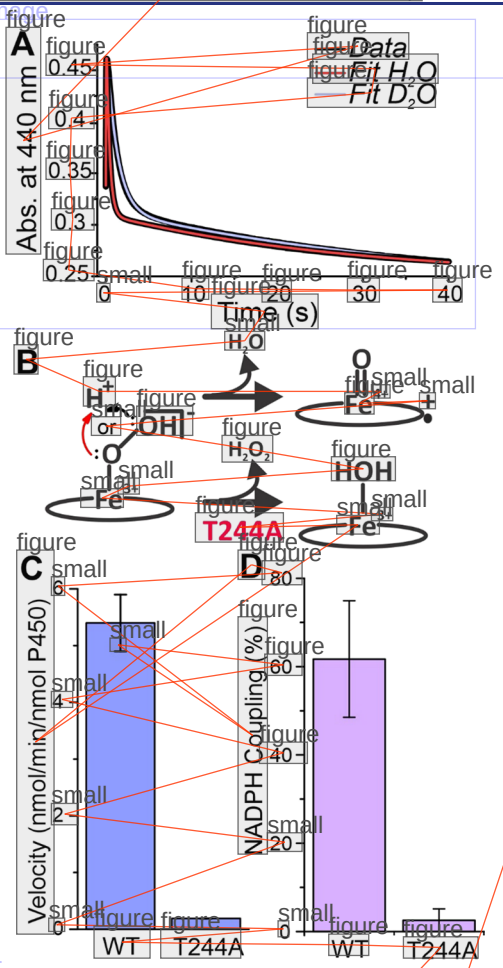

Figure 5. (A) Single-wavelength photomultiplier tube (PMT) timecourses collected at 440 nm monitoring the formation and decay of oxy for 10 μM AspB with 0.1 mM **1** (postmix concentrations) preincubated in protiated (red trace) or deuterated (blue trace) buffers. (B) Protonation of the ferric hydroperoxo at either the distal oxygen (black arrow) leading to the O-O bond cleavage and the release of water leading to CYP-I formation, or at the proximal oxygen (red arrow) leading to uncoupling and the release of hydrogen peroxide. (C) Comparison of the reaction velocities between WT (5.4 ± 0.5 nmol/min/nmol AspB) and the T244A mutant (0.19 ± 0.01 nmol/min/nmol AspB). (D) Comparison of the percent coupling of NADPH to product formation in WT (62 ± 13%) and T244A (2.6 ± 2.5%).

the inverse KSIE observed when using surrogate redox partners. This implies a change in the rate-limiting step under single turnover conditions and strongly implicates the AspB-oxy species for affecting the N-H(D) cleavage. For comparison, we performed the same experiments with **3** to determine if a KSIE is observed in autoxidation, since it has been suggested that hydrogen bonding may also play a role in the stability of the oxy complex.[36,41] However, only minor KSIEs for both phases for autoxidation were observed (k_H/k_D = 1.3 ± 0.2 and 1.4 ± 0.2 for the first and second decay phases, respectively) (Table S7). N-H abstraction by AspB-oxy would provide a proton and electron to form the ferric hydroperoxo complex. Due to the highly transient nature of this intermediate, which has only be observed in CYPs at cryogenic temperatures using cryoradiolysis and calibrated thermal annealing,[42] we were unsurprisingly unable to observe this species in stopped-flow experiments. However, to examine the role of the subsequent steps involved in downstream dimerization, we replaced the conserved threonine residue at position 244 with an alanine (T244A), which has been rigorously examined in CYPs to be crucial for maintaining correct protonation of the distal oxygen for efficient O-O bond scission to form CYP-I (Figure 5B).[24,43] CYPs that use a ferric peroxo-anion remain functional when the analogous mutation is made.[44] Compared to wild-type (WT) AspB, the rate of product formation under multiple turnover conditions is 30-fold slower in T244A (Figure 5C). Consistent with its role in proton-mediated heterolysis, the T244A mutant displays less than 3% coupling of NADPH to the product as compared to 62% in WT (Figure 5D). Furthermore, we were unable to observe any appreciable product formation in single-turnover assays with T244A AspB. This suggests a mechanism by which the conserved threonine in CYP-dimerases retains its canonical role for CYP-I formation and is critical in dimerization steps that occur after initial oxidation.

Generalization of a Superoxide-Mechanism to Other CYP DKP Dimerases. Utilizing the enzyme function initiative (EFI) suite of tools,[45] we compared the I-helix sequences of 48 CDPS-associated CYPs (Figure S18). The alcohol residue is highly conserved in these putative CYP-dimerases (typically a Ser), while the acid is replaced with aliphatic residues (typically Val or Ile). This suggests that ferric superoxide reactivity may not be limited to just AspB. To test whether the potential commonality of this mechanism to other types of DKP linkages, we evaluated the metabolic profile of NzeB, which shares ~98% sequence identity to AspB. Using the surrogate redox system, NzeB was found to convert cWP to a mixture of C-C and C-N-linked dimers as previously reported (Figure 6A).[18,19] To investigate whether C-C bond formation also

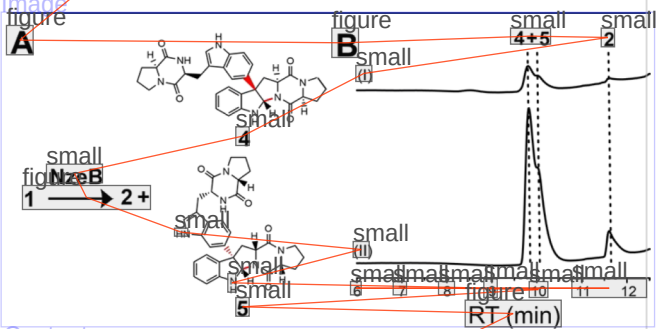

Figure 6. (A) Products of the reaction of NzeB with **1** to yield minor amounts of **2** and a mixture of (−)-naseseazine C (**4**) and (+)-naseseazine B (**5**). (B) HPLC traces of NzeB reactions utilizing only one electron equivalent and O_2 (I) or utilizing Fd and FdR (II).

proceeds via a ferric superoxide complex, we repeated single turnover experiments with NzeB. Provision of one reducing equivalent and O_2 was sufficient to generate the same ensemble of products as those formed under multiple turnover conditions with surrogate redox partners (Figure 6B, Figure S19).

DISCUSSION

Steady-state analysis of product formation by AspB has revealed a significant inverse kinetic solvent isotope effect, implicating the use of an intermediate prior to CYP-I for the initiation of substrate dimerization. The competent formation of aspergilazine A under conditions when a second electron is omitted suggests that only a single reducing equivalent from a

https://doi.org/10.1021/jacs.3c04542
J. Am. Chem. Soc. 2023, 145, 19256−19264

pubs.acs.org/JACS

redox partner is needed for catalysis to occur. Further support for the reactive nature of a ferric superoxide complex is provided through examination of the single-turnover KSIE of oxy-AspB decay, which reverts to a normal (i.e., $k_H/k_D > 1$) value due to the suppression of available proton-linked uncoupling pathways.

Unlike analogous species in nonheme mono- and di-iron enzymes,[46] the ferric-superoxide intermediate in CYPs has been largely considered catalytically inert[47] and instead serves as the primary branchpoint between uncoupling via autoxidation and further reduction and proton-mediated O-O heterolysis. One notable exception is the CYP TxtE, which catalyzes the nitration of tryptophan.[7] Transient absorption studies have shown that the ferric superoxide complex of TxtE reacts with nitric oxide (NO) gas to form a ferric peroxynitrite intermediate that subsequently undergoes a homolytic cleavage to form compound II (CYP-II) and release of an NO_2 radical.[48] Intriguingly, TxtE is also missing the conserved acid residue, which is replaced with a proline, underscoring the importance in the management of proton delivery in this process. Unlike AspB, the TxtE oxy-species is unreactive toward its substrate tryptophan but requires further "activation" by NO.[49]

The analogous oxy-species is used by the histidine-ligated heme enzyme family (recently designated as heme-dependent aromatic oxygenase (HDAO)[50]) that is historically defined by tryptophan 2,3 (TDO) and indoleamine 2,3-dioxygenases (IDO).[51−53] TDO and IDO act on a very similar tryptophan substrate, and transient absorption experiments have shown that a ferric superoxide intermediate directly reacts with the substrate through a mechanism involving direct radical addition at the C2 position of the indole ring[54] or epoxidation.[55] The heterolytic O-O cleavage then furnishes a transient compound II species[56] and a monooxygenated or epoxide product *en route* to dioxygenation.[56,57] Thus, we also considered if AspB may initiate activation of cWP in a similar manner involving a cryptic monooxygenation, but such a mechanism is inconsistent with the normal KSIE for oxy-decay upon substrate N-H deuteration and the inhibitory nature of **3**.

The apparent reactivity of the AspB-oxy complex contrasts with synthetic heme-superoxo adducts, which are typically considered sluggish oxidants for HAT. The bond dissociation free energy (BDFE) of an indole N-H bond is estimated ∼90 kcal/mol,[58] and the DKP N-H is considerably higher. Numerous reports have demonstrated HAT on relatively weak O-H (BDFE ≤80 kcal/mol) substrates,[59−62] in accordance with the limited experimental data available of the resultant hydroperoxo species (OO-H BDFE ∼70 kcal/mol). Although the precise electronic origins for enabling HAT by AspB-oxy remain to be elucidated, it is likely that preorganization of the substrate in an optimized geometry is necessary to allow for such a reaction to occur and to thwart unwanted indole oxygenation.

Based on the current findings, we propose a mechanism for AspB dimerization that is shown in Figure 7. The use of ferric-superoxide species as a primary oxidant may serve as a general stratagem to circumvent monooxygenation and forgo the nonproductive (and less controlled) oxidation of a redox-active substrate by compound I. Although the deuteration strategy employed here does not allow for precise assignment of the abstraction site (DKP vs indole N-H), the ferric-superoxide species may not have the sufficient oxidizing potential for abstraction of the DKP N-H group based on its higher bond

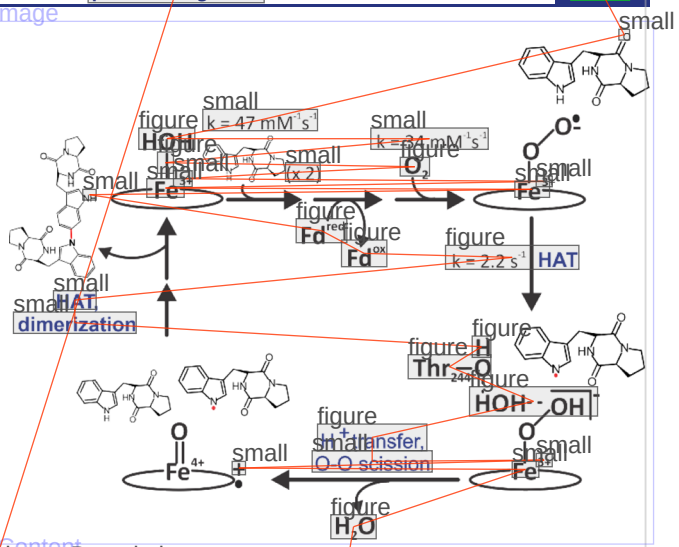

Figure 7. Proposed mechanism of cWP dimerization initiated by the ferric superoxide complex of AspB. After substrate binding, reduction to the ferrous state, and O_2 binding, the ferric superoxide species abstracts a hydrogen atom from the indole nitrogen. This furnishes a ferric-hydroperoxo complex and bypasses the need for a second reduction step. The conserved Thr244 facilitates proton delivery, enabling O-O bond scission and formation of the high-valent CYP-I. Secondary oxidation and downstream dimerization affords aspergillazine A.

dissociation energy (BDE),[58] consistent with the highly inhibitory nature observed upon substrate indole N-methylation. Indole N-H HAT would then be envisioned to furnish a hydroperoxo species, bypassing the need for the I-helix acid residue for primary protonation. As we have shown that the I-helix alcohol residue (T244) is important for functional product formation in AspB, ensuing O-O heterolysis likely occurs to give rise to compound I and provide an additional oxidizing species for the downstream secondary activation required for subsequent dimerization. HAT by compound I would yield compound II, which would then need to autodecay to regenerate the ferric water-bound resting state.

Our findings highlight a unique strategy that CYPs can use for selective diversification of natural products through C-C and C-N bond formation. This discovery not only expands the scope of CYP reactivity but may also prove valuable in leveraging these enzymes for chemoenzymatic DKP assembly. As both AspB and NzeB bypass the need for a second electron transfer step provided by a redox donor, more efficient turnover methods (e.g., light- or electrode-driven catalysis) can be envisioned to form high yields of these unique bioactive natural products.

ASSOCIATED CONTENT

Supporting Information

The Supporting Information is available free of charge at https://pubs.acs.org/doi/10.1021/jacs.3c04542.

Detailed experimental procedures and kinetic fitting parameters, Figures S1-S20 and Tables S1-S7 (PDF)

AUTHOR INFORMATION

Corresponding Author

Thomas M. Makris − *Department of Molecular and Structural Biochemistry and Department of Chemistry, North Carolina State University, Raleigh, North Carolina 27695,*

https://doi.org/10.1021/jacs.3c04542
J. Am. Chem. Soc. 2023, 145, 19256−19264

Journal of the American Chemical Society

United States; orcid.org/0000-0001-7927-620X;
Email: tmmakris@ncsu.edu

Authors

Hannah E. Gering – *Department of Molecular and Structural Biochemistry, North Carolina State University, Raleigh, North Carolina 27695, United States*

Xiaojun Li – *Department of Chemistry, North Carolina State University, Raleigh, North Carolina 27695, United States*

Haoyu Tang – *Department of Chemistry, North Carolina State University, Raleigh, North Carolina 27695, United States*

Paul D. Swartz – *Department of Molecular and Structural Biochemistry, North Carolina State University, Raleigh, North Carolina 27695, United States*

Wei-Chen Chang – *Department of Chemistry, North Carolina State University, Raleigh, North Carolina 27695, United States;* orcid.org/0000-0002-2341-9846

Complete contact information is available at: https://pubs.acs.org/10.1021/jacs.3c04542

Author Contributions

The manuscript was written through contributions of all authors. All authors have given approval to the final version of the manuscript.

Notes

The authors declare no competing financial interest.

■ ACKNOWLEDGMENTS

This work was supported by a National Institutes of Health Grants GM135315 (to T.M.M.), and GM 127588 (to W.-C.C.). This work was performed in part by the Molecular Education, Technology and Research Innovation Center (METRIC) at NC State University, which is supported by the state of North Carolina. Use of the Advanced Photon Source was supported by the US Department of Energy, Office of Basic Energy Sciences, under contract number W-31-109-Eng-38.

■ ABBREVIATIONS

CYP	cytochrome P450
DKP	diketopiperazine
SAM	radical S-adenosylmethionine
KSIE	kinetic solvent isotope effect
HAT	hydrogen atom transfer

■ REFERENCES

(1) Booker, S. J.; Lloyd, C. T. Twenty Years of Radical SAM! The Genesis of the Superfamily. *ACS Bio Med. Chem. Au* **2022**, *2*, 538−547.

(2) Bischoff, D.; Pelzer, S.; Holtzel, A.; Nicholson, G. J.; Stockert, S.; Wohlleben, W.; Jung, G.; Sussmuth, R. D. The Biosynthesis of Vancomycin-Type Glycopeptide Antibiotics-New Insights into the Cyclization Steps This work was supported by the Deutsche Forschungsgemeinschaft (SFB 323). We thank M. Schierle, Dr. S. Stevanovic and Prof. H.-G. Rammensee for help with Edman degradation and J. Turner, Prof. B. List and Prof. D. Boger (La Jolla, USA) for discussions on the work. *Angew. Chem. Int. Ed.* **2001**, *40*, 1693−1696.

(3) Forneris, C. C.; Seyedsayamdost, M. R. In Vitro Reconstitution of OxyC Activity Enables Total Chemoenzymatic Syntheses of Vancomycin Aglycone Variants. *Angew. Chem. Int. Ed.* **2018**, *57*, 8048−8052.

(4) Haslinger, K.; Maximowitsch, E.; Brieke, C.; Koch, A.; Cryle, M. J. Cytochrome P450 OxyBtei catalyzes the first phenolic coupling step in teicoplanin biosynthesis. *ChemBioChem* **2014**, *15*, 2719−2728.

(5) Mazzaferro, L. S.; Hüttel, W.; Fries, A.; Müller, M. Cytochrome P450-catalyzed regio- and stereoselective phenol coupling of fungal natural products. *J. Am. Chem. Soc.* **2015**, *137*, 12289−12295.

(6) Zhao, B.; Guengerich, F. P.; Bellamine, A.; Lamb, D. C.; Izumikawa, M.; Lei, L.; Podust, L. M.; Sundaramoorthy, M.; Kalaitzis, J. A.; Reddy, L. M.; Kelly, S. L.; Moore, B. S.; Stec, D.; Voehler, M.; Falck, J. R.; Shimada, T.; Waterman, M. R. Binding of two flaviolin substrate molecules, oxidative coupling, and crystal structure of Streptomyces coelicolor A3(2) cytochrome P450 158A2. *J. Biol. Chem.* **2005**, *280*, 11599−11607.

(7) Barry, S. M.; Kers, J. A.; Johnson, E. G.; Song, L.; Aston, P. R.; Patel, B.; Krasnoff, S. B.; Crane, B. R.; Gibson, D. M.; Loria, R.; Challis, G. L. Cytochrome P450−catalyzed L-tryptophan nitration in thaxtomin phytotoxin biosynthesis. *Nat. Chem. Biol.* **2012**, *8*, 814−816.

(8) He, F.; Mori, T.; Morita, I.; Nakamura, H.; Alblova, M.; Hoshino, S.; Awakawa, T.; Abe, I. Molecular basis for the P450-catalyzed C−N bond formation in indolactam biosynthesis. *Nat. Chem. Biol.* **2019**, *15*, 1206−1213.

(9) García-Domínguez, P.; Areal, A.; Alvarez, R.; De Lera, A. R. Chemical synthesis in competition with global genome mining and heterologous expression for the preparation of dimeric tryptophan-derived 2,5-dioxopiperazines. *Nat. Prod. Rep.* **2022**, *39*, 1172−1225.

(10) Sun, C.; Tian, W.; Lin, Z.; Qu, X. Biosynthesis of pyrroloindoline-containing natural products. *Nat. Prod. Rep.* **2022**, *39*, 1721−1765.

(11) Borthwick, A. D. 2,5-Diketopiperazines: synthesis, reactions, medicinal chemistry, and bioactive natural products. *Chem. Rev.* **2012**, *112*, 3641−3716.

(12) Martins, M. B.; Carvalho, I. Diketopiperazines: biological activity and synthesis. *Tetrahedron* **2007**, *63*, 9923−9932.

(13) Gondry, M.; Jacques, I. B.; Thai, R.; Babin, M.; Canu, N.; Seguin, J.; Belin, P.; Pernodet, J. L.; Moutiez, M. A Comprehensive Overview of the Cyclodipeptide Synthase Family Enriched with the Characterization of 32 New Enzymes. *Front. Microbiol.* **2018**, *9*, 46.

(14) James, E. D.; Knuckley, B.; Alqahtani, N.; Porwal, S.; Ban, J.; Karty, J. A.; Viswanathan, R.; Lane, A. L. Two Distinct Cyclodipeptide Synthases from a Marine Actinomycete Catalyze Biosynthesis of the Same Diketopiperazine Natural Product. *ACS Synth. Biol.* **2016**, *5*, 547−553.

(15) Saruwatari, T.; Yagishita, F.; Mino, T.; Noguchi, H.; Hotta, K.; Watanabe, K. Cytochrome P450 as dimerization catalyst in diketopiperazine alkaloid biosynthesis. *ChemBioChem* **2014**, *15*, 656−659.

(16) Yu, H.; Li, S. M. Two Cytochrome P450 Enzymes from Streptomyces sp. NRRL S-1868 Catalyze Distinct Dimerization of Tryptophan-Containing Cyclodipeptides. *Org. Lett.* **2019**, *21*, 7094−7098.

(17) Liu, J.; Xie, X.; Li, S.-M. Increasing cytochrome P450 enzyme diversity by identification of two distinct cyclodipeptide dimerases. *Chem. Commun.* **2020**, *56*, 11042−11045.

(18) Sun, C.; Luo, Z.; Zhang, W.; Tian, W.; Peng, H.; Lin, Z.; Deng, Z.; Kobe, B.; Jia, X.; Qu, X. Molecular basis of regio- and stereo-specificity in biosynthesis of bacterial heterodimeric diketopiperazines. *Nat. Commun.* **2020**, *11*, 6251.

(19) Shende, V. V.; Khatri, Y.; Newmister, S. A.; Sanders, J. N.; Lindovska, P.; Yu, F.; Doyon, T. J.; Kim, J.; Houk, K. N.; Movassaghi, M.; Sherman, D. H. Structure and Function of NzeB, a Versatile C-C and C-N Bond-Forming Diketopiperazine Dimerase. *J. Am. Chem. Soc.* **2020**, *142*, 17413−17424.

(20) Makino, M.; Sugimoto, H.; Shiro, Y.; Asamizu, S.; Onaka, H.; Nagano, S. Crystal structures and catalytic mechanism of cytochrome P450 StaP that produces the indolocarbazole skeleton. *Proc. Natl. Acad. Sci. U. S. A.* **2007**, *104*, 11591−11596.

(21) Belin, P.; Le Du, M. H.; Fielding, A.; Lequin, O.; Jacquet, M.; Charbonnier, J.-B.; Lecoq, A.; Thai, R.; Courçon, M.; Masson, C.;

Dugave, C.; Genet, R.; Pernodet, J.-L.; Gondry, M. Identification and structural basis of the reaction catalyzed by CYP121, an essential cytochrome P450 in Mycobacterium tuberculosis. *Proc. Natl. Acad. Sci. U. S. A.* **2009**, *106*, 7426−7431.

(22) Haslinger, K.; Peschke, M.; Brieke, C.; Maximowitsch, E.; Cryle, M. J. X-domain of peptide synthetases recruits oxygenases crucial for glycopeptide biosynthesis. *Nature* **2015**, *521*, 105−109.

(23) Shende, V. V.; Harris, N. R.; Sanders, J. N.; Newmister, S. A.; Khatri, Y.; Movassaghi, M.; Houk, K. N.; Sherman, D. H. Molecular Dynamics Simulations Guide Chimeragenesis and Engineered Control of Chemoselectivity in Diketopiperazine Dimerases. *Angew. Chem., Int. Ed.* **2023**, DOI: 10.1002/anie.202210254.

(24) Davydov, R.; Makris, T. M.; Kofman, V.; Werst, D. E.; Sligar, S. G.; Hoffman, B. M. Hydroxylation of camphor by reduced oxy-cytochrome P450cam: mechanistic implications of EPR and ENDOR studies of catalytic intermediates in native and mutant enzymes. *J. Am. Chem. Soc.* **2001**, *123*, 1403−1415.

(25) Denisov, I. G.; Mak, P. J.; Makris, T. M.; Sligar, S. G.; Kincaid, J. R. Resonance Raman characterization of the peroxo and hydroperoxo intermediates in cytochrome P450. *J. Phys. Chem. A* **2008**, *112*, 13172−13179.

(26) Gerber, N. C.; Sligar, S. G. A role for Asp-251 in cytochrome P-450cam oxygen activation. *J. Biol. Chem.* **1994**, *269*, 4260−4266.

(27) Nagano, S.; Poulos, T. L. Crystallographic study on the dioxygen complex of wild-type and mutant cytochrome P450cam. Implications for the dioxygen activation mechanism. *J. Biol. Chem.* **2005**, *280*, 31659−31663.

(28) Vidakovic, M.; Sligar, S. G.; Li, H.; Poulos, T. L. Understanding the role of the essential Asp251 in cytochrome p450cam using site-directed mutagenesis, crystallography, and kinetic solvent isotope effect. *Biochemistry* **1998**, *37*, 9211−9219.

(29) Aikens, J.; Sligar, S. G. Kinetic Solvent Isotope Effects during Oxygen Activation by Cytochrome P-450cam. *J. Am. Chem. Soc.* **1994**, *116*, 1143−1144.

(30) Denisov, I. G.; Sligar, S. G. Solvent isotope effects in the catalytic cycle of P450 CYP17A1: Computational modeling of the hydroxylation and lyase reactions. *J. Inorg. Biochem.* **2023**, *243*, No. 112202.

(31) Gregory, M. C.; Denisov, I. G.; Grinkova, Y. V.; Khatri, Y.; Sligar, S. G. Kinetic solvent isotope effect in human P450 CYP17A1-mediated androgen formation: evidence for a reactive peroxoanion intermediate. *J. Am. Chem. Soc.* **2013**, *135*, 16245−16247.

(32) Espinoza, R. V.; Maskeri, M. A.; Turlik, A.; Nangia, A.; Khatri, Y.; Montgomery, J.; Houk, K. N.; Sherman, D. H. Epoxidation and Late-Stage C-H Functionalization by P450 Taml Are Mediated by Variant Heme-Iron Oxidizing Species. *ACS Catal.* **2022**, *12*, 3731−3742.

(33) Wertz, D. L.; Valentine, J. S., *Nucleophilicity of Iron-Peroxo Porphyrin Complexes*. Springer Berlin Heidelberg: 2000; pp. 37−60.

(34) Peterson, J. A.; Ishimura, Y.; Griffin, B. W. Pseudomonas putida cytochrome P-450: characterization of an oxygenated form of the hemoprotein. *Arch. Biochem. Biophys.* **1972**, *149*, 197−208.

(35) Zhang, H.; Gruenke, L.; Arscott, D.; Shen, A.; Kasper, C.; Harris, D. L.; Glavanovich, M.; Johnson, R.; Waskell, L. Determination of the rate of reduction of oxyferrous cytochrome P450 2B4 by 5-deazariboflavin adenine dinucleotide T491V cytochrome P450 reductase. *Biochemistry* **2003**, *42*, 11594−11603.

(36) Clark, J. P.; Miles, C. S.; Mowat, C. G.; Walkinshaw, M. D.; Reid, G. A.; Daff, S. N.; Chapman, S. K. The role of Thr268 and Phe393 in cytochrome P450 BM3. *J. Inorg. Biochem.* **2006**, *100*, 1075−1090.

(37) Wise, C. E.; Hsieh, C. H.; Poplin, N. L.; Makris, T. M. Dioxygen Activation by the Biofuel-Generating Cytochrome P450 OleTJE. *ACS Catal.* **2018**, *8*, 9342−9352.

(38) Denisov, I. G.; Grinkova, Y. V.; Baas, B. J.; Sligar, S. G. The ferrous-dioxygen intermediate in human cytochrome P450 3A4. Substrate dependence of formation and decay kinetics. *J. Biol. Chem.* **2006**, *281*, 23313−23318.

(39) Lipscomb, J. D.; Sligar, S. G.; Namtvedt, M. J.; Gunsalus, I. C. Autooxidation and hydroxylation reactions of oxygenated cytochrome P-450cam. *J. Biol. Chem.* **1976**, *251*, 1116−1124.

(40) Tripathi, S.; Li, H.; Poulos, T. L. Structural Basis for Effector Control and Redox Partner Recognition in Cytochrome P450. *Science* **2013**, *340*, 1227−1230.

(41) Schlichting, I.; Berendzen, J.; Chu, K.; Stock, A. M.; Maves, S. A.; Benson, D. E.; Sweet, R. M.; Ringe, D.; Petsko, G. A.; Sligar, S. G. The catalytic pathway of cytochrome p450cam at atomic resolution. *Science* **2000**, *287*, 1615−1622.

(42) Denisov, I. G.; Grinkova, Y. V.; Sligar, S. G., *Cryoradiolysis and Cryospectroscopy for Studies of Heme-Oxygen Intermediates in Cytochromes P450*. Humana Press: 2012; pp. 375−391, DOI: 10.1007/978-1-61779-806-1_20.

(43) Martinis, S. A.; Atkins, W. M.; Stayton, P. S.; Sligar, S. G. A Conserved Residue of Cytochrome-P-450 Is Involved in Heme-Oxygen Stability and Activation. *J. Am. Chem. Soc.* **1989**, *111*, 9252−9253.

(44) Khatri, Y.; Gregory, M. C.; Grinkova, Y. V.; Denisov, I. G.; Sligar, S. G. Active site proton delivery and the lyase activity of human CYP17A1. *Biochem. Biophys. Res. Commun.* **2014**, *443*, 179−184.

(45) Zallot, R.; Oberg, N.; Gerlt, J. A. The EFI Web Resource for Genomic Enzymology Tools: Leveraging Protein, Genome, and Metagenome Databases to Discover Novel Enzymes and Metabolic Pathways. *Biochemistry* **2019**, *58*, 4169−4182.

(46) Bollinger, J. M., Jr.; Krebs, C. Enzymatic C-H activation by metal-superoxo intermediates. *Curr. Opin. Chem. Biol.* **2007**, *11*, 151−158.

(47) Lai, W. Z.; Shaik, S. Can Ferric-Superoxide Act as a Potential Oxidant in P450(cam)? QM/MM Investigation of Hydroxylation, Epoxidation, and Sulfoxidation. *J. Am. Chem. Soc.* **2011**, *133*, 5444−5452.

(48) Louka, S.; Barry, S. M.; Heyes, D. J.; Mubarak, M. Q. E.; Ali, H. S.; Alkhalaf, L. M.; Munro, A. W.; Scrutton, N. S.; Challis, G. L.; De Visser, S. P. Catalytic Mechanism of Aromatic Nitration by Cytochrome P450 TxtE: Involvement of a Ferric-Peroxynitrite Intermediate. *J. Am. Chem. Soc.* **2020**, *142*, 15764−15779.

(49) Martin, C. P.; Chen, M.; Martinez, M. F.; Ding, Y.; Caranto, J. D. The Ferric-Superoxo Intermediate of the TxtE Nitration Pathway Resists Reduction, Facilitating Its Reaction with Nitric Oxide. *Biochemistry* **2021**, *60*, 2436−2446.

(50) Shin, I.; Wang, Y.; Liu, A. A new regime of heme-dependent aromatic oxygenase superfamily. *Proc. Natl. Acad. Sci. U. S. A.* **2021**, *118*, No. e2106561118.

(51) Geng, J.; Liu, A. Heme-dependent dioxygenases in tryptophan oxidation. *Arch. Biochem. Biophys.* **2014**, *544*, 18−26.

(52) Basran, J.; Efimov, I.; Chauhan, N.; Thackray, S. J.; Krupa, J. L.; Eaton, G.; Griffith, G. A.; Mowat, C. G.; Handa, S.; Raven, E. L. The mechanism of formation of N-formylkynurenine by heme dioxygenases. *J. Am. Chem. Soc.* **2011**, *133*, 16251−16257.

(53) Booth, E. S.; Basran, J.; Lee, M.; Handa, S.; Raven, E. L. Substrate Oxidation by Indoleamine 2,3-Dioxygenase: Evidence for a Common Reaction Mechanism. *J. Biol. Chem.* **2015**, *290*, 30924−30930.

(54) Chung, L. W.; Li, X.; Sugimoto, H.; Shiro, Y.; Morokuma, K. Density functional theory study on a missing piece in understanding of heme chemistry: the reaction mechanism for indoleamine 2,3-dioxygenase and tryptophan 2,3-dioxygenase. *J. Am. Chem. Soc.* **2008**, *130*, 12299−12309.

(55) Capece, L.; Lewis-Ballester, A.; Batabyal, D.; Di Russo, N.; Yeh, S.-R.; Estrin, D. A.; Marti, M. A. The first step of the dioxygenation reaction carried out by tryptophan dioxygenase and indoleamine 2,3-dioxygenase as revealed by quantum mechanical/molecular mechanical studies. *J. Biol. Inorg. Chem.* **2010**, *15*, 811−823.

(56) Lewis-Ballester, A.; Batabyal, D.; Egawa, T.; Lu, C.; Lin, Y.; Marti, M. A.; Capece, L.; Estrin, D. A.; Yeh, S. R. Evidence for a ferryl intermediate in a heme-based dioxygenase. *Proc. Natl. Acad. Sci. U. S. A.* **2009**, *106*, 17371−17376.

(57) Basran, J.; Booth, E. S.; Lee, M.; Handa, S.; Raven, E. L. Analysis of Reaction Intermediates in Tryptophan 2,3-Dioxygenase: A Comparison with Indoleamine 2,3-Dioxygenase. *Biochemistry* **2016**, *55*, 6743−6750.

(58) Luo, Y.-R., *Comprehensive Handbook of Chemical Bond Energies*. 1 ed.; CRC Press: Boca Raton, 2007, DOI: 10.1201/9781420007282.

(59) Kim, H.; Rogler, P. J.; Sharma, S. K.; Schaefer, A. W.; Solomon, E. I.; Karlin, K. D. Heme-Fe(III) Superoxide, Peroxide and Hydroperoxide Thermodynamic Relationships: Fe(III)-O(2)(*-) Complex H-Atom Abstraction Reactivity. *J. Am. Chem. Soc.* **2020**, *142*, 3104−3116.

(60) Kim, H.; Rogler, P. J.; Sharma, S. K.; Schaefer, A. W.; Solomon, E. I.; Karlin, K. D. Ferric Heme Superoxide Reductive Transformations to Ferric Heme (Hydro)Peroxide Species: Spectroscopic Characterization and Thermodynamic Implications for H-Atom Transfer (HAT). *Angew. Chem.* **2021**, *60*, 5907−5912.

(61) Mondal, P.; Ishigami, I.; Gérard, E. F.; Lim, C.; Yeh, S.-R.; De Visser, S. P.; Wijeratne, G. B. Proton-coupled electron transfer reactivities of electronically divergent heme superoxide intermediates: a kinetic, thermodynamic, and theoretical study. *Chem. Sci.* **2021**, *12*, 8872−8883.

(62) Singha, A.; Dey, A. Hydrogen atom abstraction by synthetic heme ferric superoxide and hydroperoxide species. *Chem. Commun.* **2019**, *55*, 5591−5594.